J. Phys. Chem. A **2002,** *106,* 8992−8995

Rotational-Level Dependence of OH $A^2\Sigma^+$ Quenching at 242 and 196 K

Brooke L. Hemming[†] **and David R. Crosley***

Molecular Physics Laboratory, SRI International, Menlo Park, California 94025

Received: May 7, 2002; In Final Form: July 23, 2002

The rotational-level dependence of quenching of $A^2\Sigma^+$ OH has been studied below room temperature for the colliders O_2, N_2, H_2, Kr, and Xe. State-specific quenching cross sections are reported at 242 and 196 K. OH is formed over a large range of rotational levels by the photolysis of HNO_3, and the time dependence of laser-induced fluorescence decays measures the quenching. Levels as high as $N' = 13$ were studied. The quenching cross sections always decrease with increases in both N' and temperature. However, the results are ambiguous regarding a question posed earlier: Does temperature play a role in defining the rotational state dependence of OH $A^2\Sigma^+$ quenching?

Introduction

The OH radical plays a central role in the chemistry of the atmosphere. It has a very short lifetime with respect to chemical reaction, and as such, it forms an excellent test species for models of fast atmospheric photochemistry. All the source gases and radiation that control the population of OH can be measured in the same air mass as the OH itself, and estimates of long-range transport need not be considered in predictions of its concentration. Recently, several instruments capable of credible measurements have come into play in the atmospheric sciences. Several of these, including an airborne version that has flown on NASA's DC-8 in three missions,[1] are based on laser-induced fluorescence (LIF). Although these experiments are calibrated by introducing known amounts of OH as determined by flow cell chemistry or photolysis, a knowledge of quenching is important in relating observed signal sizes to system operating parameters. Moreover, because the temperature range in the troposphere, where these measurements are made, varies between approximately 200 and 300 K, the temperature dependence of quenching is also of interest.

In our laboratory, we have made measurements of quenching of $A^2\Sigma^+$ OH over a yet larger temperature range than 200 to 300 K. For lower temperatures, we have used flow cells,[2,3] for intermediate temperature, a laser pyrolysis cell,[4] and for the highest temperatures, $H_2/O_2/N_2O$ flames.[5] In all cases, the thermally averaged quenching cross sections $\sigma_Q = k_Q/v$ (where k_Q is the quenching rate coefficient and v is the average thermal velocity of the collision) decrease with increasing temperature but eventually level off. Shock tube measurements[6] at yet higher temperatures support the trend of σ_Q decreasing with increasing temperature, as do recent measurements at lower temperature.[7] This overall trend, shown for all collision partners, is attributed to the formation of a short-lived collision complex; spectroscopic studies of van der Waals complexes of OH and other gases show attractive wells in the potential surface.[8]

Moreover, it is known that, at a given temperature, σ_Q decreases as N' increases.[9,10] This in turn indicates that there are anisotropies in the potential surface so that the slowly rotating hydride more readily presents attractive wells to the collider, in contrast to a rapidly rotating collider that shows a more angularly averaged potential. This and consequences concerning the temperature dependence of the rotational dependence have been discussed.[11] There it is posited that the lower rotational levels show a sharper decline in the decrease of σ_Q with increasing temperature compared to the decline at higher N'.

In this study, we directly measure the rotational dependence of σ_Q below room temperature, viz., 242 and 196 K. Although for each N' there is generally an increase in σ_Q as the temperature decreases and for each temperature, a decreasing σ_Q as N' increases, it is not evident whether the temperature dependence of σ_Q changes differently for lower rotational levels compared with high ones.

Experimental Approach

The experiment is very similar to that in ref 12 (measurements at 300 K) except for the addition of a cooling bath. A solution of 70% HNO_3 in water and a solution of 98% aqueous H_2SO_4 are mixed in a 2:3 ratio; the sulfuric acid reduces the water vapor pressure above the mixture. This was kept at a 150-mTorr background pressure, resulting in about 5 mTorr of HNO_3. Although the acid is a rapid quencher, this small amount does not alter the useful temporal dynamic range of the quenching experiments. A 193-nm ArF laser photolyzes the nitric acid forming high N' in the OH ground state. After a delay of about 8 μs, allowing the translational degree of freedom of the OH to thermalize, selected rotational levels were elevated to the $A^2\Sigma^+$, $v' = 0$ level using a frequency-doubled excimer laser pumped dye laser. Typical pulse energies were 10 μJ in a 5-mm diameter beam. The two lasers propagated coaxially, and fluorescence was collected with an f/3 lens in a perpendicular direction. The photomultiplier was protected from room light and residual long-wavelength NO_2 chemiluminescence by Schott filters. Fluorescence decay times were monoexponential and fit between 90%

---

* Corresponding author. E-mail: david.crosley@sri.com.

[†] Also: Chemistry Department, Stanford University, Stanford, California 94305. Current address: AAAS/US EPA Fellow, Office of International Affairs, MC: 2670R, 1200 Pennsylvania Avenue, Washington, D.C. 20460.

10.1021/jp021132c CCC: $22.00

TABLE 1: k_Q (10^{-11} cm^3 s^{-1})

collider	T(K)	$N' = 2$	$N' = 4$	$N' = 6$	$N' = 7$	$N' = 8$	$N' = 10$	$N' = 12$	$N' = 13$
O_2	296[a]	12.9 ± 0.6		9.7 ± 0.7	8.9 ± 0.6				
	243	13.0 ± 0.8			9.1 ± 0.5		5.5 ± 0.3	5.0 ± 0.3	
	196	13.7 ± 0.8	12.8 ± 0.8	11.0 ± 0.7					
N_2	296	2.5 ± 0.2	2.2 ± 0.2	1.3 ± 0.4	0.5 ± 0.2				
	242	4.0 ± 0.2		1.8 ± 0.1		0.4 ± 0.3	0.2 ± 0.2		
	196	4.8 ± 0.3	3.1 ± 0.2	1.9 ± 0.1					
H_2	296	18.0 ± 0.9	15.5 ± 0.9		11.8 ± 0.7		0.1 ± 0.1		
	241	19.6 ± 1.2	15.9 ± 1.0	13.3 ± 0.8		9.6 ± 0.7	7.8 ± 0.3		
	196	19.2 ± 1.2	16.0 ± 0.9	12.2 ± 0.8					
Kr	296	6.2 ± 0.4	3.3 ± 0.3	2.1 ± 0.1			0.3 ± 0.2		
	241	6.4 ± 0.4	3.6 ± 0.2	1.9 ± 0.1			0.2 ± 0.2		
	196	5.5 ± 0.4	3.8 ± 0.3	1.8 ± 0.4					
Xe	296	17.8 ± 1.4[b]		16.2 ± 0.8			14.1 ± 1.0		10.6 ± 0.7
	242	17.4 ± 1.1	17.6 ± 1.1	16.6 ± 1.0			13.6 ± 0.8		12.1 ± 1.1
	196	17.2 ± 1.1	17.0 ± 1.0	15.5 ± 1.0		13.3 ± 0.8			

[a] All values for 296 K are taken from ref 12. [b] Value for a 300 K thermalized distribution are taken from ref 14.

TABLE 2: σ_Q (Å^2)

collider	T(K)	$N' = 2$	$N' = 4$	$N' = 6$	$N' = 7$	$N' = 8$	$N' = 10$	$N' = 12$	$N' = 13$
O_2	296[a]	17.2 ± 0.8		12.9 ± 0.9	11.9 ± 0.8				
	243	19.2 ± 1.1			13.4 ± 0.8		8.1 ± 0.5	7.4 ± 0.4	
	196	22.4 ± 1.3	21.0 ± 1.3	18.1 ± 1.1					
N_2	296	3.2 ± 0.2	3.2 ± 0.2	1.7 ± 0.5	0.6 ± 0.2				
	242	5.7 ± 0.3		2.6 ± 0.2		0.6 ± 0.4	0.1 ± 0.1		
	196	7.6 ± 0.5	5.0 ± 0.3	3.0 ± 0.2					
H_2	296	9.6 ± 0.5	8.3 ± 0.5		6.3 ± 0.4		3.6 ± 0.3		
	241	11.6 ± 0.7	9.4 ± 0.6	7.9 ± 0.5		5.7 ± 0.4	4.6 ± 0.3		
	196	12.6 ± 0.8	10.5 ± 0.6	8.0 ± 0.5					
Kr	296	9.3 ± 0.6	5.0 ± 0.4	3.1 ± 0.2			0.4 ± 0.2		
	241	10.6 ± 0.6	6.0 ± 0.4	3.2 ± 0.2			0.4 ± 0.3		
	196	11.1 ± 0.7	7.6 ± 0.5	3.7 ± 0.9					
Xe	296	27.4 ± 2.2[b]		25.1 ± 1.3			21.9 ± 1.5		16.4 ± 1.1
	242	29.9 ± 1.8	30.2 ± 1.8	28.4 ± 1.3			23.3 ± 1.4		20.8 ± 1.9
	196	32.7 ± 2.0	32.5 ± 1.9	29.5 ± 1.8		25.4 ± 1.5			

[a] All values for 296 K are taken from ref 12. [b] Value for a 300 K thermalized distribution is taken from ref 14.

and 10% of the maximum. Fluorescence lifetimes τ_{eff} were measured for six to eight collider pressures between 0 and 0.4 Torr. Three lifetimes were determined for each pressure, and the single average was used to obtain quenching rate coefficients and cross sections. A plot of $1/\tau_{\mathrm{eff}}$ against collider density furnished k_Q, which when divided by the average thermal velocity yields σ_Q. A test to ensure translational thermalization has been described in ref 12; the results showed no change in quenching as the HNO_3 density is increased. Further experimental details can be found in ref 13.

The low-temperature flow cell was constructed by enclosing a stainless steel six-way cross within a box of heavily insulated 1-in. plexiglass walls and bottom, which was filled with cold isopropanol. The isopropanol was cooled to 242 ± 2 K with a Neslab cooler and to 196 ± 1 K using a slurry of dry ice in isopropanol. The temperature was continuously monitored with a thermocouple. Previous LIF studies[3] of OH in the same cell corresponded to thermocouple measurements within the ±5% accuracy of the LIF determinations, showing that the gas in the cell had thermally equilibrated with the bath. Gas flows were controlled by mass flow meters, and collider partial pressures were taken from ratios of gas flows.

Results

Numerical results for k_Q and σ_Q are given in Tables 1 and 2, respectively. The colliders N_2 and O_2 were studied because of their importance to atmospheric monitoring of the OH radical, whereas H_2, Kr, and Xe were studied owing to fundamental interest in collision processes. The values for 296 K, needed for reference, are taken from ref 12. At the lowest temperature, 196 K, there was little signal for high N', and the measurements are only for $N' = 2$, 4, and 6, except for the Xe collider where $N' = 8$ could be excited. Graphical results are presented for the cross sections in Figures 1−5. The error bars shown in the table and the graphs are taken from the error in the plot of decay rate versus collider density and the averages of the three replicate values at each pressure, thus showing relative errors for different temperature and N'. We expect the absolute values to have this

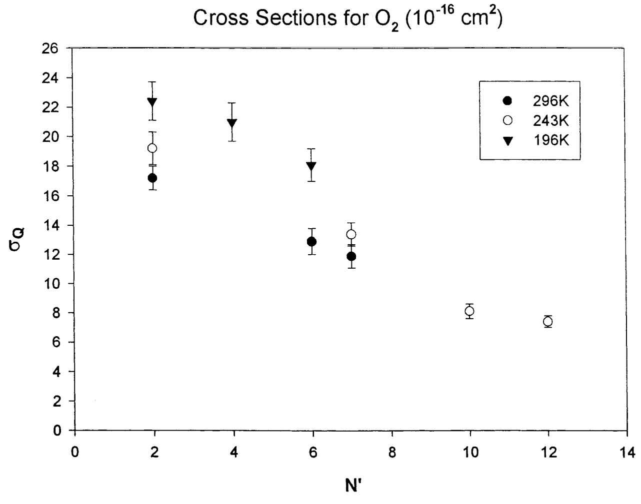

Figure 1. Quenching cross sections for an O_2 collider as a function of rotational quantum number N'. Closed circles are results at 296 K, open circles, at 242 K, and closed triangles, at 196 K.

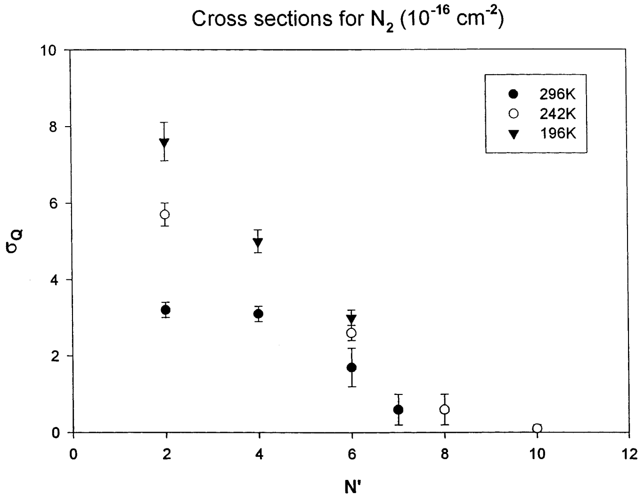

Figure 2. Quenching cross sections for a N_2 collider as a function of rotational quantum number N'. Closed circles are results at 296 K, open circles, at 242 K, and closed triangles, at 196 K.

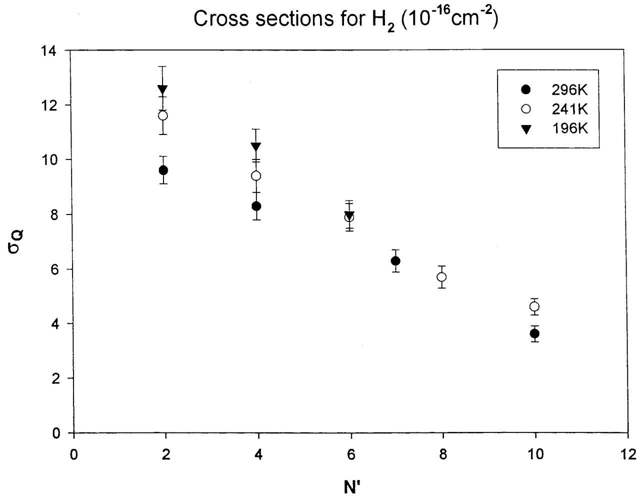

Figure 3. Quenching cross sections for a H_2 collider as a function of rotational quantum number N'. Closed circles are results at 296 K, open circles, at 242 K, and closed triangles, at 196 K.

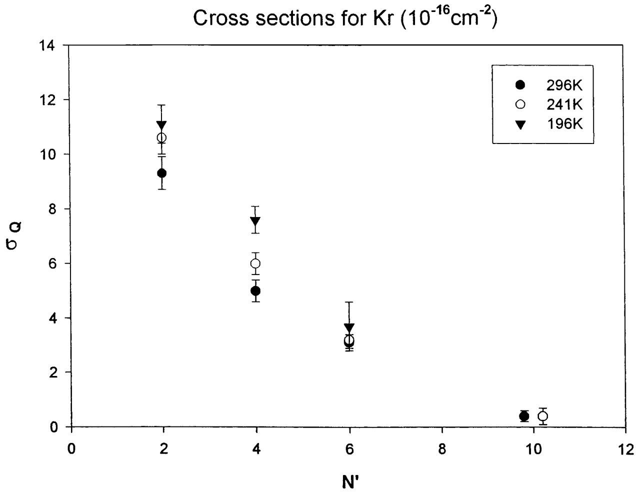

Figure 4. Quenching cross sections for a Kr collider as a function of rotational quantum number N'. Closed circles are results at 296 K, open circles, at 242 K, and closed triangles, at 196 K.

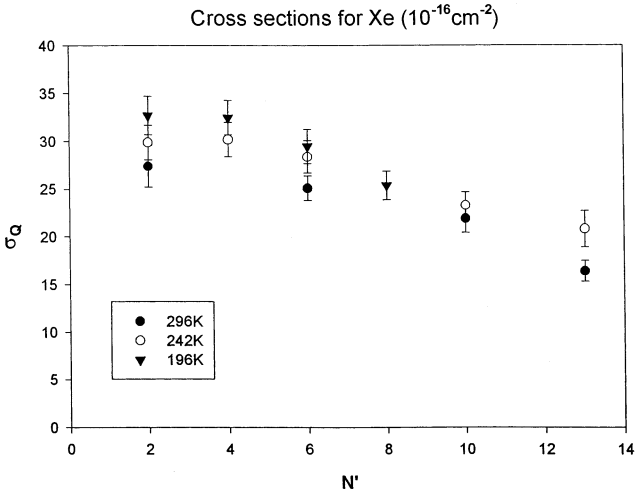

Figure 5. Quenching cross sections for a Xe collider as a function of rotational quantum number N'. Closed circles are results at 296 K, open circles, at 242 K, and closed triangles, at 196 K.

error plus about 10% (20% for the highest N' where signal levels are lower) on the basis of a previous analysis of $A^2\Sigma^+$ vibrational energy transfer measurements in the same cell.[3]

Discussion

Comparison with Previous Results. Table 3 shows relevant quenching cross sections previously measured for comparison with our $N' = 2$ values. Three of these[2,10,14] are from prior work in this laboratory, and two are from the University of Leeds.[7,15] In one SRI experiment[2] and both Leeds experiments, the $N' = 2$ level is excited, and quenching is measured predominantly for that level. In the other two SRI studies,[2,14] a bath of Ar at several Torr ensures that the intially pumped $N' = 2$ level thermalizes before significant quenching occurs. Over the temperature range of our current experiment, $N' = 2$ is always the most highly populated level, and its σ_Q should be close to the effective σ_Q of a rotationally thermal distribution.

Only in 5 cases (out of 21 total) is there disagreement beyond combined error bars: O_2 at 296 K compared with refs 2 and 15, O_2 at 296 and 242 K compared with ref 15, and N_2 at 296 and 196 K compared with ref 15. Note that the 296 K values for O_2 in refs 10 and 14, which agree within error bars with the present results, are now considered preferable to the value in ref 2 (as discussed in ref 14). We see no clear reason for the discrepancies with ref 15, but the differences are just outside the combined error bars.

Temperature-Dependent Cross Sections. σ_Q increases for all colliders and all rotational levels measured as the temperature is reduced from 296 to 242 and 196 K (although sometimes within combined or single error bars). This indicates that attractive forces are present on the OH ($A^2\Sigma^+$)-collider potential surface. It is now well established, through spectroscopic studies of Ar−OH[16] and H_2−OH[17] van der Waals complexes with the OH in the excited state, that attractive forces are important in the collision. This is confirmed by the ab initio potential surfaces calculated for the Ar−O−H combination[18] and the surfaces found in the H_2−OH interaction.[8]

This increase in σ_Q with decreasing temperature also holds for a large number of molecular colliders, as measured at temperatures near 1100 K and compared with room-temperature determinations.[4] This suggests that attractive forces are always or almost always important in the incoming channel of the collision of the partner with the OH.

The size of the cross sections, which is on the order of gas kinetic, indicates by itself the presence of attractive forces. This

TABLE 3: Comparison of σ_Q (Å^2) for $N' = 2$ with Other Literature Values

gas	T(K)	this work	ref 2	ref 10	ref 14	ref 7	ref 15
O_2	296[a]	17.2 ± 0.8	18.7 ± 1.0	20.6 ± 0.6	17.8 ± 1.2		18.6 ± 0.5
	242	19.2 ± 1.1					21.3 ± 0.6
	196	22.4 ± 1.3					23.5 ± 0.7
N_2	296	3.2 ± 0.2	4.0 ± 0.7	3.2 ± 0.5			4.3 ± 0.1
	242	5.7 ± 0.3	6.3 ± 0.6[b]				5.6 ± 0.2
	196	7.6 ± 0.5					6.8 ± 0.2
H_2	296	9.6 ± 0.5	9.2 ± 0.5	10.4 ± 0.5[c]		8.7 ± 0.7	
	241	11.6 ± 0.7	12.7 ± 0.5			10.9 ± 0.8	
	196	11.1 ± 0.7				11.8 ± 0.9	
Kr	296	9.3 ± 0.6			8.3 ± 0.7	8.5 ± 0.6	
	242	10.6 ± 0.6					
	196	11.1 ± 0.7				11.6 ± 0.8	

[a] All values at 296 K are taken from ref 12. [b] Extrapolated. [c] Interpolated.

is especially interesting in the cases of H_2, Kr, and Xe, which are simple enough species that ab initio potential energy surface calculations may be feasible in the future.

***J*-Dependent Cross Sections.** The σ_Q are also found, for all colliders studied, to decrease with increasing rotational level. This is also true for vibrational energy transfer in OH.[19] This trend is ascribed[19] to an anisotropic attractive surface (which is evident in the ab initio calculations[18]). As the OH rotates faster, the collision partner during the approach sees a surface with less anisotropy, and the entrance channel pathway is less dominated by the deep wells found at some approach angles.

Temperature-Dependent *J* Dependence? One might think from the above discussion that the J dependence should be enhanced at lower temperatures, which correspond to lower collision energies. At smaller approach velocities, the partner would more susceptible to the washing out of the anisotropy by a more rapidly rotating OH. σ_Q for OH colliding with H_2O was observed to follow this behavior between 1000 and 2300 K in $CH_4/O_2/N_2O$ flames.[5] Comparing the flame values with those at room temperature[10] confirms the conclusion.

The limited temperature range of these experiments, combined with the size of the error bars at higher rotational level, makes it impossible to discern a combined temperature−rotational dependence for quenching. Furthermore, the general inability to access very high rotational levels (e.g., $J' = 20.5$) prevented confirmation in this experiment of the existence of an independent rate at high J rotational levels, as seen in ref 12, although trends are evident in the data presented here. Therefore, we cannot confirm or contradict the existence of a changing J dependence of σ_Q as the temperature is lowered or an independence at high J' and low temperature.

Acknowledgment. We thank Jorge Luque, Gregory Smith, and Leah Williams for many valuable discussions. This work was supported by the Global Tropospheric Experiment of the National Aeronautics and Space Administration and by the Atmospheric Chemistry Divison of the National Science Foundation.

References and Notes

(1) Tan, D.; Faloona, I.; Simpas, J. B.; Brune, W.; Olson, J.; Crawford, J.; Sandholm, S.; Guan, H.-W.; Vaughn, T.; Mastromarino, J.; Sachse, G.; Vay, S.; Podolske, J.; Averg, M.; Heikes, B.; Snow, J.; Singh, H. *J. Geophys. Res.* **2001**, *32*, 667.

(2) Copeland, R. A.; Crosley, D. R. *J. Chem. Phys*. **1986**, *84*, 3099.

(3) Steffens, K.; Crosley, D. R. *J. Chem. Phys*. **2000**, *112*, 9427.

(4) Fairchild, P. W.; Smith, G. P.; Crosley, D. R. *J. Chem. Phys*. **1983**, *79*, 1795.

(5) Jeffries, J. B.; Kohse-Höinghaus, K.; Smith, G. P.; Copeland, R. A.; Crosley, D. R. *Chem. Phys. Lett*. **1988**, *152*, 160.

(6) Paul, P. H.; Durant, J. L.; Gray, J. A.; Furnaletto, M. R. *J. Chem. Phys*. **1995**, *102*, 8378.

(7) Heard, D. E.; Anderson, D. A. *Phys. Chem. Chem. Phys*. **2000**, *2*, 67.

(8) Lester, M. I.; Loomis, R. A.; Schwartz, R. L.; Walch, S. P. *J. Phys. Chem*. **1997**, *101*, 9195.

(9) McDermid, I. S.; Laudenslager, J. B. *J. Chem. Phys*. **1982**, *76*, 1824.

(10) Copeland, R. A.; Dyer, M. J.; Crosley, D. R. *J. Chem. Phys*. **1985**, *82*, 4022.

(11) Crosley, D. R. *J. Phys. Chem*. **1989**, *93*, 6273.

(12) Hemming, B. L.; Crosley, D. R.; Harrington, J. E.; Sick, V. *J. Chem. Phys*. **2001**, *115*, 3099.

(13) Hemming, B. L. Ph.D. Thesis, Stanford University, Stanford, CA, June 1998.

(14) Wysong, I. J.; Jeffries, J. B.; Crosley, D. R. *J. Chem. Phys*. **1990**, *92*, 5218.

(15) Bailey, A. E.; Heard, D. E.; Paul, P. H.; Pilling, M. J. *J. Chem. Soc., Faraday Trans*. **1997**, *93*, 2915.

(16) Berry, M. T.; Brustein, M. R.; Adamo, J. R.; Lester, M. I. *J. Phys. Chem*. **1988**, *92*, 5551.

(17) Loomis, R. A.; Lester, M. I. *J. Chem. Phys*. **1995**, *104*, 4371.

(18) Degli-Esposti, A.; Werner, H.-J. *J. Chem. Phys*. **1990**, *93*, 3351.

(19) Lengel, R. K.; Crosley, D. R. *J. Chem. Phys*. **1978**, *68*, 5309.